CFSRC COLLOQUIUM

Proceedings of the Cold-Formed Steel Research Consortium Colloquium
20-22 October 2020 (cfsrc.org)

Numerical Study of Double Stud LSF Walls Exposed to Fire Conditions

Harikrishnan Magarabooshanam[1], Anthony D. Ariyanayagam[2], Mahen Mahendran[3]

Abstract

Fire safety of light gauge steel frame (LSF) stud walls is important in the design of buildings. Many experimental and numerical studies have been undertaken to investigate the fire performance of load bearing LSF walls under standard fire conditions. Single stud LSF walls are the most common configuration used in the residential sector for both load bearing and non-load bearing walls. But in places where higher acoustic insulation rating and load carrying capacities are required, double stud LSF walls are used. Double stud walls have two parallel rows of studs with studs located directly opposite each other. Standard fire tests of full-scale double stud walls have shown that their fire resistance level (FRL) is superior to that of single stud walls. In single stud LSF walls the major mode of heat transfer from fire side to the ambient side is by conduction through steel studs followed by convection and radiation within the cavity whereas in the case of double stud LSF walls the conduction through steel studs is significantly reduced by the air gap between the two rows of stud. In this study, numerical models were developed to simulate this complex heat transfer mechanism in the double stud LSF walls and to explain the reasons for the superior fire resistance of double stud walls. Thermal numerical analysis results were compared with full-scale standard fire test results. This paper presents the details of the numerical study of load bearing double stud walls, comparisons with fire test results and its findings.

1. Introduction

Experimental investigation on LSF walls under fire conditions can be used to determine the FRL under different load ratios. However, the experimental approach is time consuming and expensive. To overcome this shortcoming, numerical methods are used to predict the same. This paper focuses on developing a robust thermal model to predict the temperature distribution in double stud LSF wall in fire. Several numerical models using Finite Element (FE) techniques have been developed by past researchers to simulate the heat transfer in single stud LSF walls [1–3]. This includes 2D and 3D models using different FE software packages. Majority of the thermal FE models assumed the heat transfer by conduction through plasterboards and studs from fire side to the ambient side. The cavity region was assumed to be closed and corresponding boundary conditions were specified in the FE model. Cavity radiation was considered as the predominant mode of heat transfer within the cavity to simulate the heat transfer mechanism in LSF walls [3,4]. However, this assumption holds good only to LSF walls with single row of studs as the stud flanges are in contact with the adjoining plasterboard. Also, the previous models were created by considering a closed cavity which does not precisely represent the experimental fire tests. These assumptions did not significantly affect the time-temperature curves due to the presence of single row of studs resulting in a continuous contact within the cavity from fire side to the ambient side in previous research studies. However, in the case of complex LSF walls such as double stud LSF walls, there prevails a discontinuous stud arrangement, resulting in a different heat transfer mechanism within the cavity in comparison with single stud LSF wall. Therefore, to address these issues, a detailed literature review was first undertaken and the most suitable thermal models were considered to predict the temperature profiles of the conducted full-scale fire tests in [5]. The developed numerical model was then used to perform thermal analysis for all the conducted full-scale fire tests on double stud LSF walls to predict the time-temperature curves of studs and plasterboards. The predicted time-temperature curves of stud hot and cold flanges were then used to validate against the conducted full-scale fire tests.

2. Thermal Modelling of Double Stud LSF Walls in FDS

To develop the thermal model of double stud LSF walls, the following full-scale fire tests were considered from [5] and are summarised in Table 1. Figures 1 and 2 show the plan view of typical double stud LSF walls with 70 and 90 mm

[1] PhD researcher, School of Civil & Environmental Engineering, Queensland University of Technology, harikrishnan.magarabooshanam@hdr.qut.edu.au
[2] Lecturer, School of Civil & Environmental Engineering, Queensland University of Technology, a.ariyanayagam@.qut.edu.au
[3] Professor, School of Civil & Environmental Engineering, Queensland University of Technology, m.mahendran@.qut.edu.au

studs considered for thermal numerical model development in this paper.

Table 1: Full-scale fire tests of double stud walls considered for numerical model development

Test Name	Stud depth (mm)	Stud Thickness (mm)	Cavity depth (mm)
T1	90	0.95	200
T2	90	0.75	200
T4	70	0.95	160

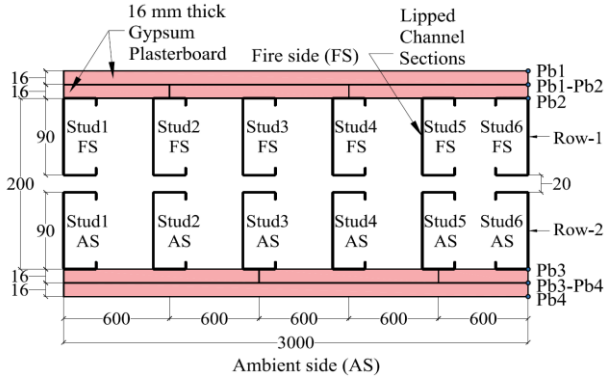

Figure 1: Plan view of full-scale fire Tests-T1 and T2 [5] considered for numerical model

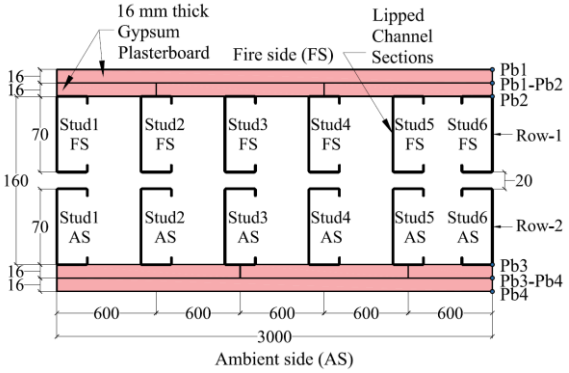

Figure 2: Plan view of full-scale fire Test-T4 [5] considered for numerical model

Unlike other FE packages in which the thermal models of LSF walls are readily available, very limited literature is available on the thermal models of LSF walls developed in computational fluid dynamic software Fire Dynamics Simulator (FDS) except in research studies conducted by [6,7]. The previous FDS model considered in the literature assumed the LSF wall as a homogenous entity and the thermal models were created with single obstruction (&OBST) comprising of studs and plasterboards. However, this approach cannot be employed in this study as the individual time-temperature curves from the studs are necessary to predict the structural behaviour of the LSF wall in fire. Therefore, the plasterboards and studs were modelled separately to depict the experimental set-up.

Past literature considered different model dimensions based on their experimental set-up. The model dimensions varied form 50 x 50 mm to 3 x 3 m. Likewise, the mesh density also varied from 5 to 50 mm ([6,7]). This assumption was best suitable as the time-temperature curves were measured on the fire exposed and ambient sides in the above-mentioned research studies. However, these studies did not model the structural behaviour of the wall. To develop the current thermal model based on past literature, a sensitivity analysis was conducted initially to determine the effects of the model dimensions. Also, in the sensitivity analyses the obstructions (&OBST) were modelled as solid entity, which was found to add complexity to the model resulting in higher computational time. Therefore, a simplistic approach of modelling the obstructions as 2D entity was chosen in this research study to model the complex LSF walls.

2.1 Thermal model description in FDS

The models were created in the command line interface using Notepad++, a general-purpose text editor. However, PyroSim was used for pre-processing the models in certain instances to consolidate meshes in the boundary. SmokeView was used for post-processing and visualising the thermal model results. Outputs from the thermal models were saved to a CSV file, which were later used for plotting the time-temperature curves. Certain assumptions were used in creating the FDS thermal model. The models were created with the appropriate depth of the test wall used in the experiments. However, the height and width of the model were restricted to 200 mm.

The variation in heat transfer along the height of the test wall was ignored to simplify the model. This is because, the standard time-temperature curve is specified as the input boundary condition to the entire fire exposed surface (Pb1) using the vent function (&VENT) in FDS. This implies that, the temperature input is uniform throughout the surface and the variation in temperature which occurs in the experiments due to difference in furnace burner temperatures can be assumed insignificant and ignored in the current model, as the comparison is made against the average time-temperature curve achieved in the furnace. It is to be noted that the ISO 834 time-temperature curve is specified as the input boundary condition on the fire side plasterboard in ABAQUS and SAFIR thermal models. However, in FDS it is specified through a &VENT surface, which provides the leverage to simulate the standard fire curve from furnace similar to the full-scale fire tests. This might result in a small difference between the incident fire side plasterboard (Pb1) temperature and the standard fire curve due to the small distance between the &VENT surface and the Pb1 surface. This small difference in temperatures will still be within the permissible limit of 100°C as per AS 1530.4 and

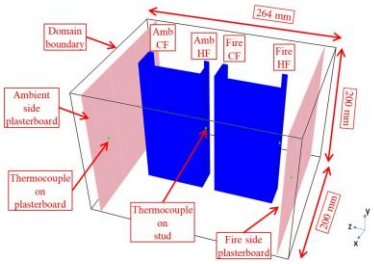

Figure 3: FDS model of Double Stud LSF wall panel

Considering the above-mentioned findings, the obstructions in the model followed ``1 cell thick" rule of FDS as shown in Figure 3. The temperature dependent material properties for gypsum plasterboards, steel studs and glass fibre insulation for the thermal analysis were taken from past research studies [8]. The temperature dependent material properties were used for conductivity and specific heat only. Temperature-dependant material properties were specified to the model using &RAMP function in the FDS input file. The density was kept constant at 768.5kg/m^3 for plasterboard and 7850 kg/m^3 for steel. An emissivity of 0.9 was used for the plasterboards while the emissivity used for the steel stud was 0.7. The model was enclosed in a domain boundary with 16 mm mesh based on the sensitivity analyses, matching the plasterboard thickness. This is to accommodate the plasterboard thickness and to facilitate the measurement of temperatures between plasterboard interface (Pb1-Pb2 and Pb3-Pb4). Convective heat transfer co-efficient of 25 W/m^2°C was considered for the fire side plasterboard surface while it was 10 W/m^2°C for the ambient side plasterboard surface.

AS 1530.4 standard fire curve [9] (identical to ISO834 curve [10]) was specified as the input boundary condition to replicate the fire side using &VENT function. The domain boundary was created in close contact with the model to prevent any heat loss around the model sides during simulation. The domain boundary was closed in all directions and adiabatic boundary conditions were specified representing no heat transfer through the sides. The boundary facing the ambient side was alone kept open to simulate the natural convection from the ambient side plasterboard surface. As “1-cell thick” modelling technique was used, the contact between the studs and plasterboards was achieved by specifying the material thickness of plasterboard and studs. The corresponding thickness was specified on the surface line using the &SURF function. Temperatures were measured across the model using the &DEVC function at various locations similar to thermocouples and the corresponding time-temperature curves were plotted. The thermal model analysis was carried out for a time period of 240 min for all the conducted full-scale fire test configurations. The time-temperature curves from the FDS model and experiment are compared and discussed in the next section.

3. Thermal analysis results

The thermal model was created with its height and width of 200 mm while its depth of the model was 264 mm similar to the full-scale fire Test-T1.

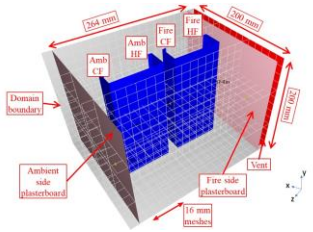

Figure 4: Thermal model of Test-T1 wall

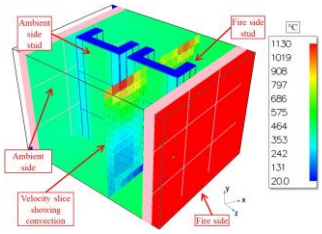

Figure 5: Output from FDS thermal analysis

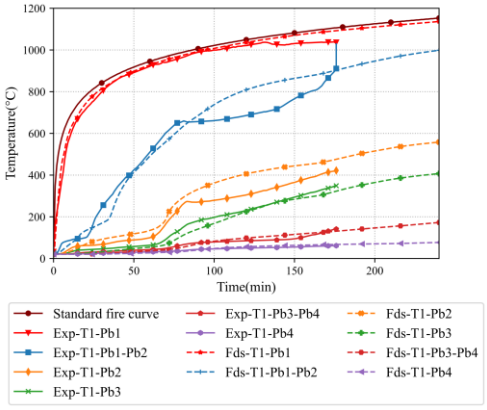

(a)

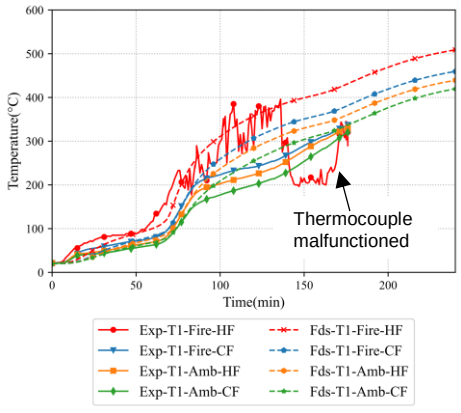

(b)

Figure 6: Comparison of Time-Temperature Curves from Experiment and FDS model for Test-T1 90 x 0.95 mm Double Stud Wall (a) Average Plasterboard (b) Stud4-Mid

3.1 Model validation

The thermal analysis was carried out for a time period of 240 min. Figure 4 shows the thermal model of Test-T1 with 16 mm meshes. The boundary domain was subdivided to nine regions to facilitate parallel processing in the HPC cluster. Through this the thermal model could be solved in 26 min, which is a considerable optimisation in the computational time.

Temperature profile and velocity slice from FDS thermal model are shown in Figure 5. Time-temperature curves of plasterboard from FDS thermal analysis are compared against experimental results and are presented in Figure 6. Notations for surfaces such as Pb1, Pb1-Pb2, Stud1, Stud2, etc as used in these figures are based on Figures 1 and 2. Fire side time-temperature curve (Fds-T1-Pb1) exhibited good agreement with the ISO 834 time-temperature curve. Plasterboard interface time-temperature curve (Fds-T1-Pb1-Pb2) exhibited a reasonable agreement with the experimental results till 75 min of fire test. The plateau region experienced in the fire test time-temperature curve was not significantly noticeable in the FDS thermal analysis prediction. The occurrence of plateau region in the plasterboard interface is attributed to the factors such as wider cavity depth, natural convection together with radiation effects, discontinuous stud arrangement, and moisture movement within the plasterboard. Except for the effects of moisture movement, all the other effects were accounted for in the current thermal model. However, the combined effects along with the moisture movement between the plasterboard interface could not be simulated due to the complexity in the modelling technique and is beyond the scope of this research study. But, the model was able to successfully incorporate the effects of convection within the cavity due to the change in the air temperature within the cavity. This is evident from the time-temperature curve of fire side plasterboard interface surfaces as shown in Figure 6(a). This confirms that the developed FDS model could better predict the thermal behaviour of non-cavity insulated double stud LSF walls. The time-temperature curve of the fire side cavity surface from the thermal model (Fds-T1-Pb2) was higher than the experimental curve. However, the ambient side cavity (Pb3), the ambient side plasterboard interface (Pb3-Pb4) and the ambient side plasterboard surface time-temperature curve predictions exhibited reasonable agreement with the experimental results.

Stud time-temperature curves shown in Figure 6(b) also exhibited good agreement with the experimental results till 75 min of the fire test. The increase in slope experienced in the time-temperature curves from 50 min of the experimental results could also be simulated by the developed thermal model with reasonable accuracy. However, as the predicted fire side cavity (Pb2) plasterboard temperatures were higher than those in the experiments (Figure 6(b)), similar effects were noticeable in the stud hot and cold flanges wherein the predicted hot and cold flange time-temperature curves were marginally higher than the experimental results. The maximum temperature recorded by the fire side hot flange on Stud4-Mid (Exp-T1-Fire-HF) at the end of the fire test at 176 min was 395°degree C while the predictions from FDS thermal model was 431°C. i.e., a difference of 8.35% (36°C). This can be considered as small in relation to the use of stud hot flange temperatures in structural failure time predictions.

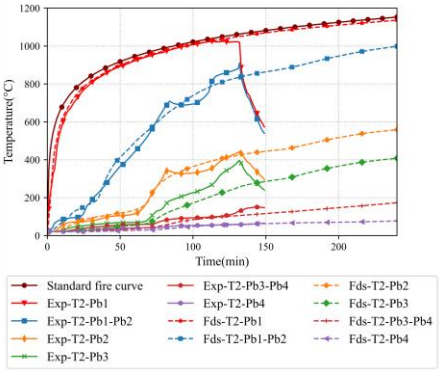

(a)

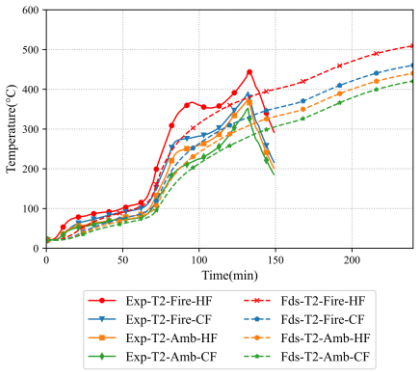

(b)

Figure 7: Comparison of Time-Temperature Curves from Experiment and FDS model for Test-T2 90 x 0.75 mm Double Stud Wall (a) Average Plasterboard (b) Stud4-Mid

Figure 7 (a) compares the plasterboard time-temperature curves for Test-T2 of a double stud wall made of 90 x 0.75 mm studs with a load ratio of 0.4. The plasterboard time-temperature curves exhibited reasonable agreement except for T2-Pb3 where the FDS model predictions were less than the experimental results. However, the ambient side plasterboard surface time-temperature curves also agreed reasonably well. Stud time-temperature curves agreed well till 60 min of the fire test as shown in Figure 7 (b). The steep increase experienced in the Exp-T2-Fire-HF could not be simulated in the FDS model as this was a result of localised plasterboard open-up in the fire test. The temperature recorded at 132 min in Exp-T2-Fire-HF was 444°C while it was 380°C from the FDS model, i.e., FDS model prediction

of the stud hot flange temperature was 64°C less than the experimental results. Similarly, the difference in the fire side cold temperature was 62°C (393-331°C). The fire side hot and cold flange temperatures are 14.4% and 15.77% less than the corresponding experimental results of Test-T2. This may be partly due to the plasterboard fall-off on the fire side plasterboard during the fire test as reported in [5].

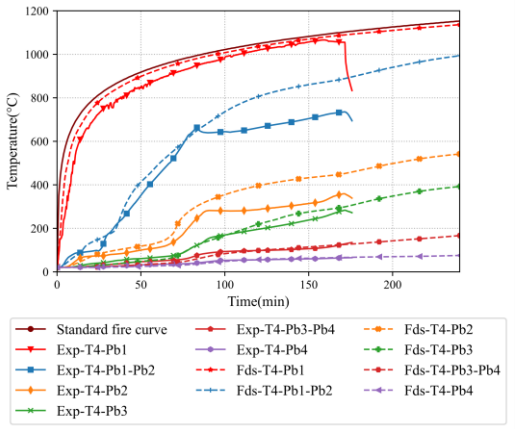

(a)

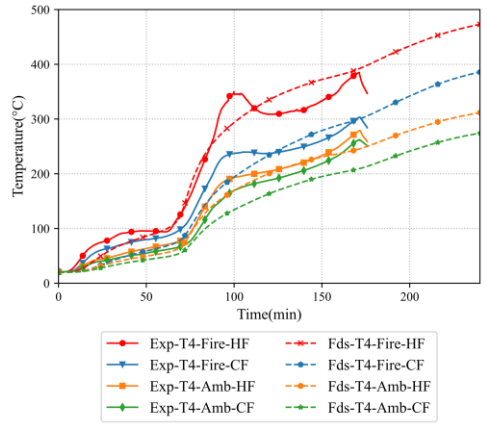

(b)

Figure 8: Comparison of Time-Temperature Curves from Experiment and FDS model for Test-T4 70 x 0.95 mm Double Stud Wall (a) Average Plasterboard (b) Stud4-Mid

Test-T4 was conducted on a double stud wall made of 70 x 0.95 mm studs under a load ratio of 0.4. Figure 8(a) compares the plasterboard time-temperature curves from FDS thermal analysis and experiment. The plasterboard time-temperature curves predicted by the FDS thermal model were higher than the experimental results from Test-T4 till the fire side cavity surface. However, the ambient side plasterboard time-temperature curves matched reasonably well with the experimental results. Stud hot and cold flange time-temperature curves shown in Figure 8(b) also exhibited good agreement. The ambient side hot and cold flange time-temperature curves from FDS thermal analysis (Fds-T4-Amb-HF and CF) were marginally less in comparison with the experimental results (Exp-T4-Amb-HF and CF).

3.2 Effect of plasterboard open-up

As plasterboard open-up was noticeable in all the fire tests, it becomes a necessity to include these effects to simulate the sudden rise in time-temperature curves. To determine the effect of the size of plasterboard open-up on the time-temperature curves from the thermal model, double stud wall Test-T1 model was investigated with an open-up size 67 x 67 mm pertaining to one third of the plasterboard size in the model. It was used in all the FDS thermal models throughout this paper based on a sensitivity study.

In the present model the plasterboard open-up is considered by removing the middle portion for simplification. To achieve the plasterboard open-up effect on FDS thermal model, the concept of ``set-point'' temperature was used in the fire side plasterboard interface (Pb1-Pb2). Once the thermocouple Pb1-Pb2 reaches the set point temperature a portion of the plasterboard (67 mm x 67 mm) was removed during the analysis and the thermal analysis was continued till 240 min with a hole in the fire side plasterboard. A “set-point” temperature of 900°C was used at the plasterboard interface (Pb1-Pb2) to initiate the plasterboard open-up based on STP 1588 [9].

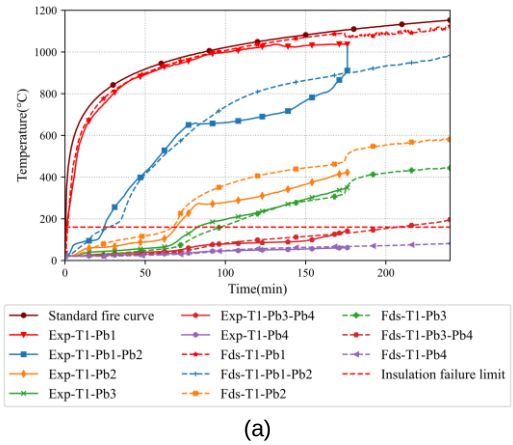

(a)

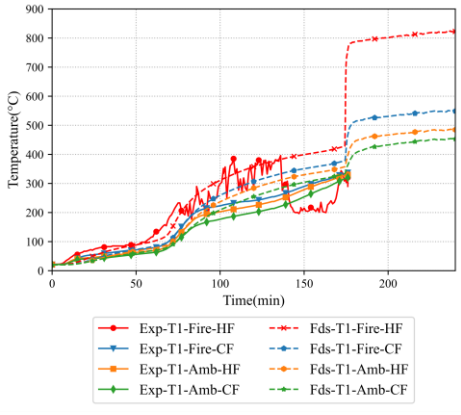

(b)

Figure 9: Comparison of Time-Temperature Curves from Experiment and FDS Model with Plasterboard Open-Up for Test-T1 (a) Average Plasterboard (b) Stud4-Mid

Figures 9(a) and (b) show the plasterboard and stud time-temperature curves from FDS thermal model with plasterboard open-up for double stud wall Test-T1. The sudden increase in the plasterboard time-temperature curve at 176 min can be simulated reasonably as shown in Figure 9(a). This sudden increase is also noticeable in the stud time-temperature curves comparison shown in Figure 9 (b). The fire side hot flange temperatures also agree reasonably well with the experimental results which will be used in the structural FE model for predicting the failure time of the wall configuration.

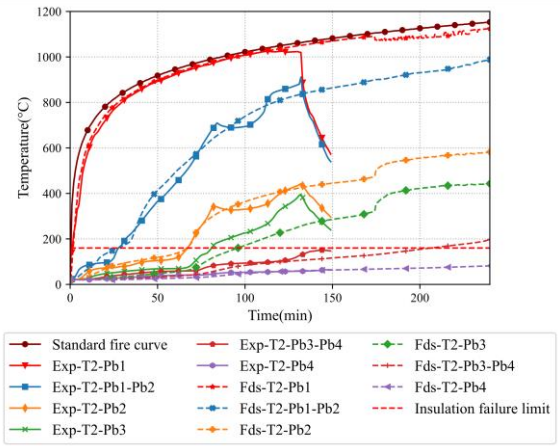

(a)

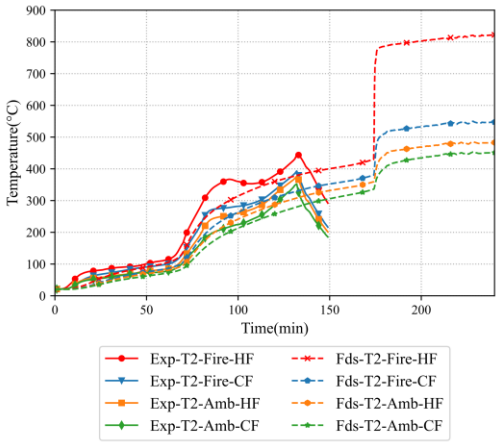

(b)

Figure 10: Comparison of Time-Temperature Curves from Experiment and FDS Model with Plasterboard Open-Up for Test-T2 (a) Average Plasterboard (b) Stud4-Mid

Figure 10 shows the time-temperature curve comparison for Test-T2. The sudden increase in the plasterboard time-temperature curve as shown in Figure 10(a) was noticeable from 120 min. However, the FDS thermal model predictions shows the sudden increase after 175 min. This is reflected in the stud time-temperature curves also as shown in Figure 10(b). The delay in sudden temperature rise in the hot flange may lead to increased structural failure time which may lead to unconservative results. Test-T2 was conducted with 0.75 mm thick studs unlike Test-T1 with 0.95 mm studs. The set-point temperature of 900°C may be higher for thinner stud sections of Tests-T2 in comparison with Tests-T1. This was because of the use of thinner studs in the test wall. Severe plasterboard fall-off was also observed in Test-T2 causing premature failure and was discussed in [5]. Also, during fire tests under load bearing conditions, the furnace is stopped once the test wall fails due to structural inadequacy criterion. The time-temperature curves of plasterboard and studs dip after this time and is evident by the cooling face of the time-temperature curves as shown in Figure 10(a). However, the FDS models are analysed for a time period of 240 min. The behaviour of the test wall post-fire test can be determined through this which will help in determining the structural failure time of the test wall under different load ratios.

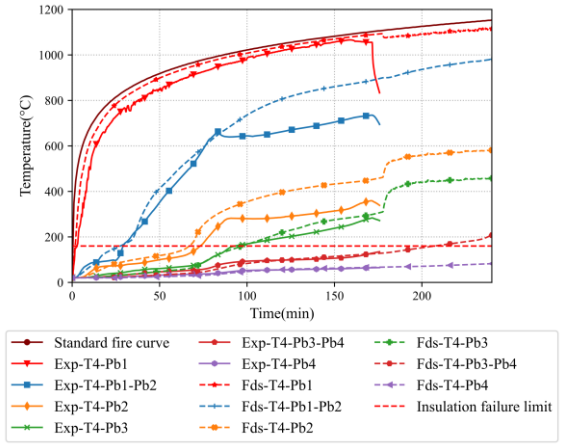

(a)

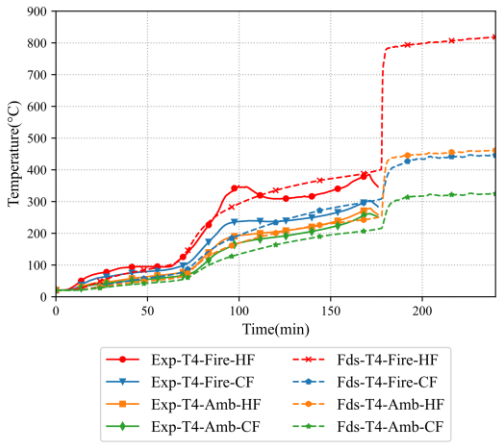

(b)

Figure 11: Comparison of Time-Temperature Curves from Experiment and FDS Model with Plasterboard Open-Up for Test-T4 (a) Average Plasterboard (b) Stud4-Mid

The FDS thermal model results for double stud wall Test-T4 with 70 x 0.95 mm studs are presented in Figure 11. Plasterboard open-up was noticeable at the test wall failure time of 171 min for Test-T4 from the FDS thermal analysis results. FDS thermal model was able to predict the open-up

time to a reasonable accuracy and is noticeable by the sudden increase in the plasterboard time-temperature curve after 175 min in Figure 11(a). The sudden increase in the stud time-temperature curves was also evident in the FDS model predictions and is shown in Figure 11(b). Test-T4 was conducted on 70 x 0.95 mm studs and the time-temperature curves of the plasterboards and studs match reasonably well considering 900°C as the set-point temperature. Due to the absence of other research data on the plasterboard fall-off set-point temperature, conservatively the set-point temperature proposed in STP 1588 by [11] was adopted throughout this research.

4. Conclusions

A detailed numerical study of double stud LSF walls in fire was conducted using thermal computational fluid dynamic techniques with the help of FDS and the results were compared with experimental results reported in [5]. Following conclusions are drawn from this study.

- 3D thermal models were created in FDS using ``1-cell thick'' rule and the time-temperature curves were predicted for all the full-scale fire tests.
- The shortcomings in the SAFIR and ABAQUS thermal FE models as observed in other studies such as simulating the effects of convection within the cavity was addressed in the FDS thermal model.
- Previous ABAQUS models considered apparent thermal properties to simulate the plasterboard open-up in cavity insulated LSF walls. However, this technique was inadequate in simulating the sudden increase in the plasterboard and stud time-temperature curves. This issue was also addressed in the developed FDS thermal model, wherein a portion (67 mm x 67 mm) of the plasterboard was removed based on a given set-point temperature.
- The plasterboard removal technique could simulate the steep rise in the time-temperature curve experienced in the non-cavity insulated double stud LSF walls with reasonably accuracy.

5. Acknowledgments

The authors would like to thank QUT, Australian Research Council and National Association of Steel Framed Housing (NASH) for providing research facilities, financial support and test materials for this study and Senior Technicians, Barry Hume and Glenn Atlee, for their assistance with the fire tests.

References

[1] Feng, M., Wang, Y.C. and Davies, J.M. (2003). “Thermal performance of cold-formed thin-walled steel panel systems in fire”. In: Fire Safety Journal 38.4, pp. 365–394.

[2] Keerthan, P. and M. Mahendran, M. (2012). “Numerical modelling of non-load-bearing light gauge cold-formed steel frame walls under fire conditions”. In: Journal of Fire Sciences 30.5, pp. 375–403.

[3] Ariyanayagam, A. D. and Mahendran, M. (2019). “Influence of cavity insulation on the fire resistance of light gauge steel framed walls”. In: Construction and Building Materials 203, pp. 687–710.

[4] Rusthi, M., Keerthan, P., Mahendran, M. and Ariyanayagam, A.d. (2017). “Investigating the fire performance of LSF wall systems using finite element analyses”. In: Journal of Structural Fire Engineering 8.4, pp. 354–376.

[5] Magarabooshanam, H., Ariyanayagam, A.D and Mahendran, M. “Behaviour of load bearing double stud LSF walls in fire,” Fire Safety Journal, vol. 107, pp. 15–28, Jul. 2019.

[6] L´azaro, D., E. Puente, M. L´azaro, P. G. L´azaro, and J. Pe˜na (2016). “Thermal modelling of gypsum plasterboard assemblies exposed to standard fire tests”. In: Fire and Materials 40.4, pp. 568–585.

[7] Nguyen, Q. T., T. Ngo, P. Tran, P. Mendis, L. Aye, and S. K. Baduge (2018). “Fire resistance of a prefabricated bushfire bunker using aerated concrete panels”. In: Construction and Building Materials 174, pp. 410–420.

[8] Dodangoda, M. T. (2018). “Improving the fire resistance of cold-formed steel frame wall systems using enhanced plasterboards”. PhD thesis. Queensland University of Technology.

[9] SA (2014). AS 1530.4 - Methods for fire tests on building materials, components and structures, Part 4: Fire-resistance test of elements of construction.

[10] ISO 834 (2014). ISO 834-11:2014. Fire resistance tests – Elements of building construction – Part 11: Specific requirements for the assessment of fire protection to structural steel elements.

[11] Sultan, M. A. (2015). “Effect of Gypsum Board Orientation on Board Fall-Off in Fire Resistance Test Assemblies”. In: Advances in Gypsum Technologies and Building Systems, ASTM STP1588, pp. 10–29.